

## Mixed Convection of the Stagnation-point Flow Towards a Stretching Vertical Permeable Sheet

Anuar Ishak<sup>1\*</sup>, Roslinda Nazar<sup>1</sup>, Norihan M. Arifin<sup>2</sup> & Ioan Pop<sup>3</sup>

<sup>1</sup>*School of Mathematical Sciences, Universiti Kebangsaan Malaysia,  
43600 UKM Bangi, Selangor, Malaysia*

<sup>2</sup>*Department of Mathematics, Universiti Putra Malaysia,  
43400 UPM Serdang, Selangor, Malaysia*

<sup>3</sup>*Faculty of Mathematics, University of Cluj, R-3400 Cluj, CP 253, Romania*

### ABSTRACT

An analysis was done for the steady two-dimensional stagnation-point mixed convection flow of an incompressible viscous fluid towards a stretching vertical permeable sheet in its own plane. The stretching velocity and the surface temperature are assumed to vary linearly with the distance from the stagnation-point. Two equal and opposite forces are impulsively applied along the  $x$ -axis so that the wall is stretched, keeping the origin fixed in a viscous fluid of constant ambient temperature. The transformed boundary layer equations were solved numerically for some values of the parameters considered using an implicit finite difference scheme known as the Keller-box method. Flow and heat transfer characteristics were analyzed and discussed. Both cases of the assisting and opposing flows were considered and it was found that dual solutions exist for the opposing flow, whereas a unique solution resulted for the assisting flow.

**Keywords:** Boundary layer, heat transfer, mixed convection, permeable sheet, stagnation-point flow, stretching sheet

### INTRODUCTION

The flow near a stagnation point has attracted many investigations during the past several decades because of its wide applications in many practical applications such as cooling of electronic devices by fans, cooling of nuclear reactors, and many hydrodynamic processes. Hiemenz (1911) was the first to study the two-dimensional stagnation-point flow, and obtained an exact similarity solution of the governing Navier-Stokes equations. Since then many investigators have considered various aspects of such flow, and obtained closed-form analytical as well as numerical solutions. Ramachandran *et al.* (1988) studied laminar mixed convection in two-dimensional stagnation flows around heated surfaces by considering both cases of an arbitrary wall temperature and arbitrary surface heat flux variations. They found that a reverse flow developed in the buoyancy opposing flow region, and dual solutions are found to exist for a certain range of the buoyancy parameter. This work was then extended by Devi *et al.* (1991) for the unsteady case, and by Lok *et al.* (2005) for a vertical surface immersed in a micropolar fluid. Dual solutions were found to exist by these authors for a certain range of buoyancy parameter.

---

\* Corresponding Author

E-mail: anuarishak2007@yahoo.co.jp

All of the above-mentioned investigations considered the flow impinging normally to a vertical or horizontal surface at rest. The stagnation point flows toward a surface which is moved or stretched, have been considered for example by Chiam (1994, 1996), Mahapatra and Gupta (2001, 2002), Nazar *et al.* (2004a,b) and more recently by Ishak *et al.* (2006a,b, 2007a). The aim of this study was to extend the work by Ishak *et al.* (2006b) for the case of a permeable surface. A thorough review on the flow and heat transfer over a permeable stretching surface can be found in Gupta and Gupta (1977), Dutta (1989), Watanabe (1991), and Magyari and Keller (2000). In the actual manufacturing process, the stretched surface speed and temperature play an important role in the cooling process. Furthermore, during the manufacture of plastic and rubber sheets, it is often necessary to blow a gaseous medium through the not-yet-solidified material. The study of flow field and heat transfer is necessary for determining the quality of the final products.

### PROBLEM FORMULATION AND BASIC EQUATIONS

Consider the stagnation flow of an incompressible viscous fluid normal to a vertical plate as shown in Fig. 1. It is assumed that the ambient fluid is moved with a velocity  $u_e(x) = ax$  in the  $y$ -direction towards the stagnation point on the plate, where  $a$  is a constant and  $a \geq 0$ . It is also assumed that the surface is stretched in the  $x$ -direction such that the  $x$ -component of the velocity and temperature vary linearly along it, i.e.  $u_w(x) = bx$  and  $T_w(x) = T_\infty + cx$ , respectively, where  $b (>0)$  and  $c$  are arbitrary constants. Under these assumptions along with the Boussinesq and boundary layer approximations, the system of equations which model the boundary layer flow are given by

$$\frac{\partial u}{\partial x} + \frac{\partial v}{\partial y} = 0, \quad (1)$$

$$u \frac{\partial u}{\partial x} + v \frac{\partial u}{\partial y} = u_e \frac{du_e}{dx} + \nu \frac{\partial^2 u}{\partial y^2} \pm g\beta(T - T_\infty), \quad (2)$$

$$u \frac{\partial T}{\partial x} + v \frac{\partial T}{\partial y} = \alpha \frac{\partial^2 T}{\partial y^2}, \quad (3)$$

where  $u$  and  $v$  are the velocity components along the  $x$  and  $y$  axes, respectively,  $T$  is the fluid temperature,  $g$  is the gravity acceleration,  $\alpha$ ,  $\nu$  and  $\beta$  are the thermal diffusivity, kinematic viscosity and thermal expansion coefficients, respectively. The last term on the right-hand side of Eq. (2) represents the influence of the thermal buoyancy force, with “+” and “-” signs pertaining to the buoyancy assisting and opposing flow regions, respectively. Fig. 1 illustrates such a flow field for a vertical, heated surface with the upper half of the flow field being assisted and the lower half of the flow field being opposed by the buoyancy force. The reverse trend will occur if the plate is cooled below the ambient temperature. The reported results are thus true for both the heated and cooled surface conditions when the

appropriate (assisting and opposing) flow regions are selected (see Ramachandran *et al.* (1988)). We shall assume that the boundary conditions of Eqs. (1) – (3) are

$$\begin{aligned} v = V_w, u = u_w(x), T = T_w(x) \quad \text{at } y = 0, \\ u \rightarrow u_e(x), T \rightarrow T_\infty \quad \text{as } y \rightarrow \infty. \end{aligned} \tag{4}$$

In order for similarity solutions to exist,  $V_w$  has to be of the form (see Gupta and Gupta (1977), Dutta (1989) and Ishak *et al.* (2007b,c,d,e,f))

$$V_w = -(bv)^{1/2} \gamma, \tag{5}$$

where  $\gamma = f(0)$ , with  $\gamma > (0)$  is for mass suction and  $\gamma < (0)$  is for mass injection. The continuity equation can be satisfied by introducing a stream function  $\psi$  such that

$$u = \frac{\partial \psi}{\partial y}, \quad v = -\frac{\partial \psi}{\partial x}. \tag{6}$$

The momentum and energy equations can be transformed to the corresponding ordinary differential equations by the following substitutions:

$$\eta = \left(\frac{b}{v}\right)^{1/2} y, \quad f(\eta) = \frac{\psi}{(bv)^{1/2} x}, \quad \theta(\eta) = \frac{T - T_\infty}{T_w - T_\infty}. \tag{7}$$

The transformed ordinary differential equations are:

$$f''' + ff'' - f'^2 + \varepsilon^2 + \lambda\theta = 0, \tag{8}$$

$$\frac{1}{Pr} \theta'' + f\theta' - f'\theta = 0, \tag{9}$$

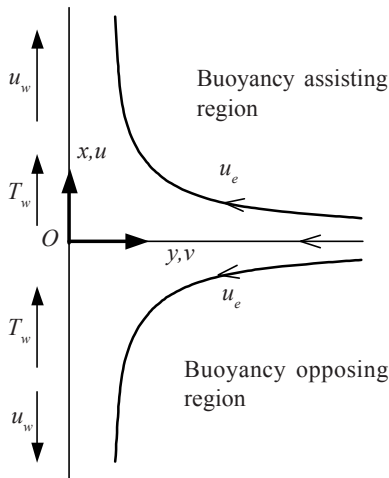


Fig. 1: Physical model and coordinate system

subject to the boundary conditions (4) which become

$$\begin{aligned} f(0) &= \gamma, \quad f'(0) = 1, \quad \theta(0) = 1, \\ f'(\infty) &\rightarrow \varepsilon, \quad \theta(\infty) \rightarrow 0, \end{aligned} \tag{10}$$

where  $\varepsilon = a/b$ , primes denote differentiation with respect to  $\eta$ ,  $Pr$  is the Prandtl number and the constant  $\lambda$  is the buoyancy or mixed convection parameter defined as

$$\lambda = \pm \frac{Gr_x}{Re_x^{1/2}}, \tag{11}$$

with the “ $\pm$ ” sign having the same meaning as in Eq. (2). Further,  $Gr_x = g\beta(T_w - T_\infty)x^3/\nu^2$  is the local Grashof number and  $Re_x = u_w x/\nu$  is the local Reynolds number. It should be noticed that  $\lambda > 0$  and  $\lambda < 0$  correspond to the assisting and opposing buoyant flows, respectively. When  $\lambda = 0$  and  $\varepsilon = 1$ , the solution of Eq. (8) subject to the boundary conditions is given by

$$f(\eta) = \eta + \gamma. \tag{12}$$

The physical quantities of interest are the skin friction coefficient  $C_f$  and the local Nusselt number  $Nu_x$ , which are defined as

$$C_f = \frac{\tau_w}{\rho u_w^2 / 2}, \quad Nu_x = \frac{xq_w}{k(T_w - T_\infty)}, \tag{13}$$

respectively, where the skin friction  $\tau_w$  and the heat transfer from the plate  $q_w$  are given by

$$\tau_w = \mu \left( \frac{\partial u}{\partial y} \right)_{y=0}, \quad q_w = -k \left( \frac{\partial T}{\partial y} \right)_{y=0}, \tag{14}$$

with  $\mu$  and  $k$  being the dynamic viscosity and thermal conductivity, respectively. Using the non-dimensional variables (7), we get

$$\frac{1}{2} C_f Re_x^{1/2} = f''(0), \quad Nu_x / Re_x^{1/2} = -\theta'(0). \tag{15}$$

Equations (8) and (9) subject to the boundary conditions (10) are solved numerically by an implicit finite difference scheme. To support the validity of the numerical method used, we get approximate solutions of Eqs. (8) and (9) subject to the boundary conditions (10) valid for small values of  $\varepsilon$ . By investigating the terms in the governing equation, we assume that the solution of Eqs. (8) and (9) near  $\varepsilon = 0$  is of the form

$$f(\eta) = \sum_{i=0}^{\infty} f_i(\eta) \varepsilon^i, \quad \theta(\eta) = \sum_{i=0}^{\infty} \theta_i(\eta) \varepsilon^i, \tag{16}$$

where  $f_i$  and  $\theta_i$  are the perturbations in  $f$  and  $\theta$ , respectively. Substituting expressions (16) into Eqs. (8) and (9), and comparing the like terms of  $\varepsilon$  gives the following set of equations:

$$\begin{aligned}
 f_0''' + f_0 f_0'' - f_0'^2 + \lambda \theta_0 &= 0, \\
 \frac{1}{Pr} \theta_0'' + f_0 \theta_0' - f_0 \theta_{0i} &= 0,
 \end{aligned}
 \tag{17}$$

and

$$\begin{aligned}
 f_i''' + \sum_{j=0}^i f_j f_{i-j}'' - 2f_0' f_i' + \delta_{i2} + \lambda \theta_i &= 0, \\
 \frac{1}{Pr} \theta_i'' + \sum_{j=0}^i f_j \theta_{i-j}' - \sum_{j=0}^i f_j' \theta_{i-j} &= 0,
 \end{aligned}
 \tag{18}$$

for  $i \geq 1$ , subject to the boundary conditions

$$\begin{aligned}
 f_i(0) = \delta_{i0} f_0, \quad f_i'(0) = \delta_{i0}, \quad \theta_i(0) = \delta_{i0} \\
 f_i'(\infty) \rightarrow \delta_{i1}, \quad \theta_i(\infty) \rightarrow 0,
 \end{aligned}
 \tag{19}$$

for  $i \geq 0$ , where  $\delta_{ij}$  is the delta Kronecker, which is defined by

$$\delta_{ij} = \begin{cases} 1 & \text{if } i = j \\ 0 & \text{if } i \neq j \end{cases}$$

The skin friction coefficient and the local Nusselt number (15) are approximately given now, respectively, by

$$\begin{aligned}
 \frac{1}{2} C_f \text{Re}_x^{1/2} &= f_0''(0) + f_1''(0)\epsilon + f_2''(0)\epsilon^2, \\
 Nu_x / \text{Re}_x^{1/2} &= -[\theta_0'(0) + \theta_1'(0)\epsilon + \theta_2'(0)\epsilon^2].
 \end{aligned}
 \tag{20}$$

### RESULTS AND DISCUSSION

Equations (8) and (9) subject to the boundary conditions (10) were solved numerically using the Keller-box method, which is described in Cebeci and Bradshaw (1988). The results shown are for a study on the influences of several non-dimensional parameters. The results of the skin friction coefficient, local Nusselt number, velocity and temperature distributions are illustrated in graphs, while the values of the skin friction coefficient and the local Nusselt number for some parameters are given in tables.

Tables 1 and 2 show the values of the skin friction coefficient and the local Nusselt number, respectively, for certain values of the related parameters. The values of the skin friction coefficient  $f''(0)$  obtained in this study are compared with those of Mahapatra and Gupta (2002) and Nazar *et al.* (2004a,b), while the values of the local Nusselt number  $-\theta'(0)$  which represent the heat transfer rate at the surface are compared with those of Ali (1995). The comparisons revealed good agreement.

TABLE 1  
The values of  $f''(0)$  for various values of  $\varepsilon$  when  $Pr = 1$ ,  $\lambda = 0$  and  $\gamma = 0$

$\varepsilon$	Mahapatra and Gupta (2002)	Nazar et al. (2004a)	Nazar et al. (2004b)	Result of this study
0.01	-	-0.9980	-0.9980	-0.9980
0.10	-0.9694	-0.9694	-0.9694	-0.9694
0.20	-0.9181	-0.9181	-0.9181	-0.9181
0.50	-0.6673	-0.6673	-0.6673	-0.6673
2.00	2.0175	2.0176	2.0175	2.0175
3.00	4.7293	4.7296	4.7296	4.7294
10.00	-	36.2687	36.2687	36.2603

TABLE 2  
The values of  $-\theta'(0)$  for various values of  $\gamma$  and  $Pr$  when  $\varepsilon = 0$  and  $\lambda = 0$

$\gamma$	Results of Ali (1995)			Results of this study		
	$Pr = 0.72$	$Pr = 1$	$Pr = 10$	$Pr = 0.72$	$Pr = 1$	$Pr = 10$
-1.0	0.5436738	0.6167397	0.9404818	0.5455	0.6181	0.9418
-0.6	0.6322861	0.7420708	1.4674400	0.6345	0.7441	1.4709
-0.4	0.6679058	0.8076850	1.9593240	0.6866	0.8198	1.9681
-0.2	0.7417784	0.9018322	2.6984210	0.7446	0.9050	2.7096
0.0	0.8055581	0.9959655	3.7004690	0.8088	1.0000	3.7208
0.2	0.8758492	1.0999160	4.9436630	0.8798	1.1050	4.9765
0.4	0.9529272	1.2135290	6.3735120	0.9575	1.2198	6.4260
0.6	1.0364530	1.3364480	7.9392070	1.0420	1.3440	8.0178
1.0	-	-	-	1.2297	1.6180	11.4762

Therefore, the code that was developed can be used with high confidence to study the problem discussed in this paper. Moreover, to support the validity of the numerical method used, the governing equations (8)-(10) were solved by using series expansion that are valid for small values of the velocity ratio parameter  $\varepsilon$  ( $= a/b$ ). The values of  $f''(0)$  and  $-\theta'(0)$  obtained by using both methods are shown in Tables 3 and 4, respectively. The results show excellent agreement for small  $\varepsilon$ . The values of  $-\theta'(0)$  as shown in Tables 2 and 4 are always positive. This follows from the integral relationship  $-\theta'(0) = 2 Pr \int_0^\infty f' \theta d\eta$  which is obtained from Eqs. (9) and (10). Furthermore, the local Nusselt number as shown in Table 2 increases with  $Pr$ . This is a result of the decreasing thermal boundary layer thickness which implies an increase in the wall temperature gradient.

Fig. 2a shows the numerical results of the dimensionless skin friction coefficient for various values of the suction/injection parameter  $\gamma$  when  $Pr = 1$  and  $\varepsilon = 1$ , while the respective local Nusselt number are presented in Fig. 2b. It is seen from Fig. 2a that for  $Pr = 1$  and  $\varepsilon = 1$ , the values of  $f''(0)$  are positive for the assisting flow ( $\lambda > 0$ ), and negative for the opposing flow ( $\lambda < 0$ ). Physically, a positive sign of  $f''(0)$  implies that the fluid exerts a

TABLE 3  
The values of  $f''(0)$  for various values of  $\varepsilon$  and  $\lambda$  when  $Pr = 1$  and  $\gamma = 0$

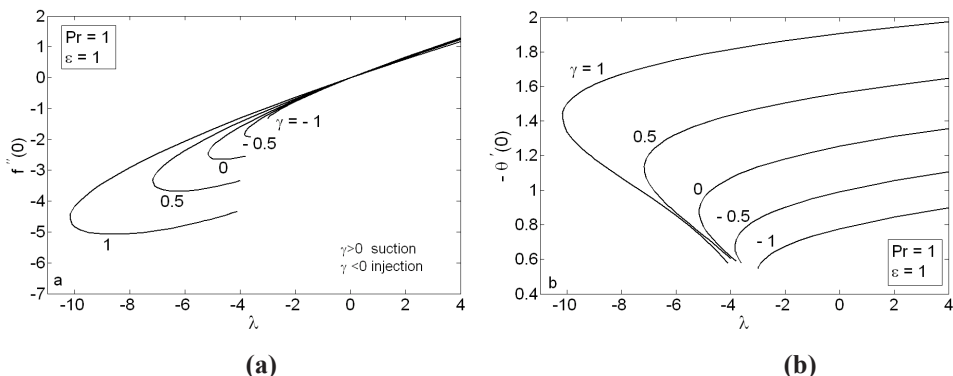
$\varepsilon$	Numerical Eq. (15)			Small $\varepsilon$ Eq. (20)		
	$\lambda = -0.1$	$\lambda = 1$	$\lambda = 10$	$\lambda = -0.1$	$\lambda = 1$	$\lambda = 10$
0	-1.0513	-0.5608	2.3042	-1.0513	-0.5608	2.3042
0.01	-1.0490	-0.5596	2.3050	-1.0488	-0.5595	2.3050
0.05	-1.0372	-0.5528	2.3095	-1.0335	-0.5514	2.3102
0.1	-1.0176	-0.5398	2.3178	-1.0022	-0.5343	2.3207
0.2	-0.9638	-0.5002	2.3432	-0.8997	-0.4769	2.3547
0.5	-0.7075	-0.2846	2.4887			
1	-0.0343	0.3350	2.9495			
2	1.9899	2.2913	4.5884			
5	11.7331	11.9449	13.6462			

TABLE 4  
The values of  $-\theta'(0)$  for various values of  $\varepsilon$  and  $\lambda$  when  $Pr = 1$  and  $\gamma = 0$

$\varepsilon$	Numerical Eq. (15)			Small $\varepsilon$ Eq. (20)		
	$\lambda = -0.1$	$\lambda = 1$	$\lambda = 10$	$\lambda = -0.71$	$\lambda = 1$	$\lambda = 10$
0	0.9856	1.0873	1.3716	0.9856	1.0873	1.3716
0.01	0.9880	1.0881	1.3719	0.9881	1.0882	1.3719
0.05	0.9977	1.0921	1.3734	1.0013	1.0931	1.3737
0.1	1.0079	1.0982	1.3757	1.0250	1.1024	1.3769
0.2	1.0362	1.1133	1.3813	1.0963	1.1312	1.3862
0.5	1.1186	1.1714	1.4058	1.5016	1.2999	1.4382
1	1.2502	1.2827	1.4646			
2	1.4855	1.5020	1.6154			
5	2.0418	2.0473	2.0899			

drag force on the sheet and a negative sign implies the opposite. Moreover, all curves intersect at a point where  $\lambda = 0$ , i.e. when the buoyancy force is absent. The value of  $f''(0)$  at this point is zero. This is not surprising since Eqs. (8) and (9) are uncoupled when  $\lambda = 0$ , and the stretching velocity is equal to the ambient fluid velocity when  $\varepsilon = 1$ , which implies skin friction  $\tau_w = 0$ . This result is in agreement with the exact solution (12), which implies  $f''(\eta) = 0$ , for all  $\eta$ . In contrast, Fig. 2b shows that there are heat transfers from the sheet to the fluid even when the skin friction is zero. This is because the sheet and the fluid are of different temperatures. Figs. 2a and 2b show the existence of dual solutions for a certain range of  $\lambda < 0$  (opposing flow). The solution for a particular value of  $\gamma$  exists up to a critical value of  $\lambda$  (say  $\lambda_c$ ). Beyond this value, the boundary layer separated from the surface, thus we are unable to get the solution using the boundary layer approximations. To proceed with the solution, the full Navier-Stokes equations have to be solved. It is evident from Figs. 2a

and  $2b$  that suction delays the boundary layer separation, while injection accelerates it. The curve bifurcates at  $\lambda = \lambda_c$ , and the lower branch solution continues further and terminates at a certain value of  $\lambda$ . It should be remarked that the computations have been performed until the point where the solution did not converge, and the calculations were terminated at that point. *Figs. 3a* and *3b* depict the velocity and temperature profiles for selected values of the parameters, which support the existence of dual solutions shown in *Figs. 2a* and *2b*.



*Fig. 2: (a) Variations of  $f''(0)$ ; (b) Variations of  $-\theta'(0)$ , as a function of  $\lambda$  at selected values of  $\gamma$  when  $Pr = 1$  and  $\epsilon = 1$*

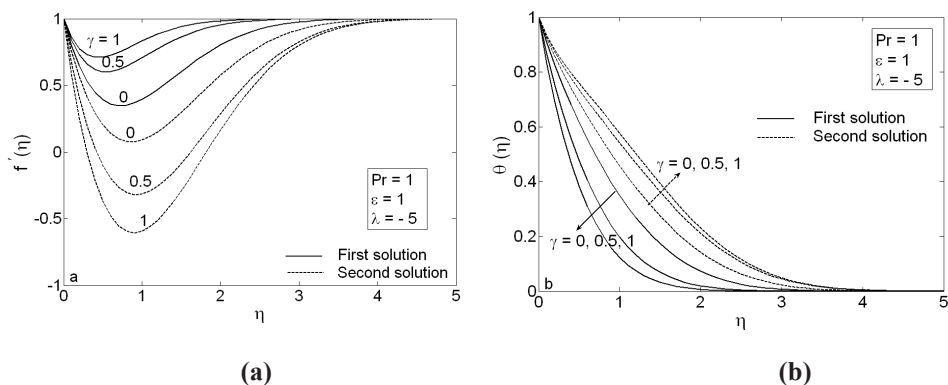


*Fig. 3: (a) Velocity profiles  $f'(\eta)$ ; (b) Temperature profiles  $\theta(\eta)$ , for various values of  $\gamma$  when  $Pr = 1, \epsilon = 1$  and  $\lambda = -5$*

*Figs. 4a* and *4b* show the velocity and temperature profiles for selected values of  $\epsilon$  when  $Pr = 1$  and  $\lambda = 1$ . *Fig. 4a*, shows that when  $\epsilon > 1$ , the flow has a boundary layer structure and the thickness of the boundary layer decreases with increase in  $\epsilon$ . According to Mahapatra and Gupta (2002), for a fixed value of  $b$  corresponding to the stretching of the surface, an increase in  $a$  in relation to  $b$  (such that  $a/b > 1$ ) implies an increase in the straining motion near the stagnation region resulting in increased acceleration of the external stream, and this leads to the thinning of the boundary layer with an increase in  $\epsilon$ . Further, *Fig. 4a* shows that when  $\epsilon < 1$ , the flow has an inverted boundary layer structure. This is a



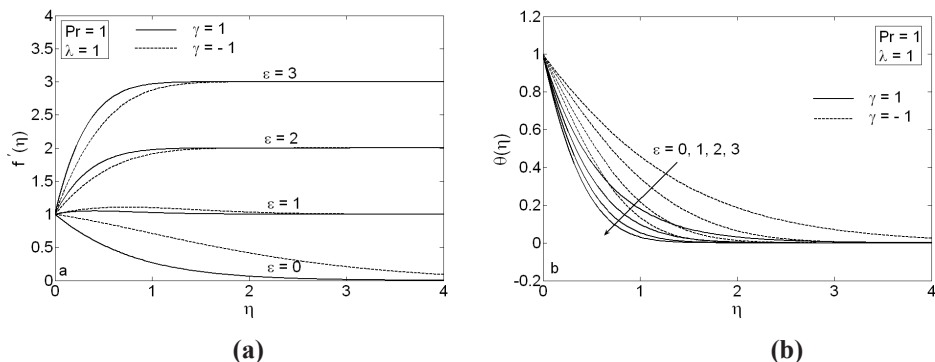


Fig. 4: (a) Velocity profiles  $f'(\eta)$ ; (b) Temperature profiles  $\theta(\eta)$ , for various values of  $\epsilon$  when  $Pr = 1$  and  $\lambda = 1$

result from the fact that when  $\epsilon < 1$ , the stretching velocity,  $bx$ , of the surface exceeds the velocity,  $ax$ , of the external stream. Figs. 3 and 4 show that the boundary conditions (10) are satisfied, which supports the validity of the results of this study.

### CONCLUSIONS

This study concerned the theory of the problem of stagnation-point flow and heat transfer towards a stretching vertical permeable sheet immersed in a viscous and incompressible fluid. The governing boundary layer equations were solved numerically using an implicit finite difference method. Both the skin friction coefficient and the local Nusselt number increase with increasing buoyancy effects. Suction increases the heat transfer from the surface, whereas injection causes a decrease. Moreover, suction delays the boundary layer separation, while injection acts in the opposite. Dual solutions were found to exist for the opposing flow, and Prandtl number enhances the heat transfer rate at the surface.

### ACKNOWLEDGEMENTS

This work is supported by a research grant (SAGA fund: STGL-013-2006) from the Academy of Sciences Malaysia.

### REFERENCES

ALI, M.E. 1995. On thermal boundary layer on a power-law stretched surface with suction or injection. *Int. J. Heat Fluid Flow* 16: 280-290.

CEBECI, T. and P. BRADSHAW. 1988. *Physical and Computational Aspects of Convective Heat Transfer*. New York: Springer.

CHIAM, T.C. 1994. Stagnation-point flow towards a stretching plate. *J. Phys. Soc. Japan* 63: 2443-2444.

CHIAM, T.C. 1996. Heat transfer with variable conductivity in a stagnation-point flow towards a stretching sheet. *Int. Comm. Heat Mass Trans.* 23: 239-248.

- DEVI, C.D.S., H.S. TAKHAR and G. NATH. 1991. Unsteady mixed convectin flow in stagnation region adjacent to a vertical surface. *Heat Mass Trans.* 26: 71-79.
- DUTTA, B.K. 1989. Heat transfer from a stretching sheet with uniform suction and blowing. *Acta Mech.* 78: 255-262.
- GUPTA, P.S. and A.S. GUPTA. 1977. Heat and mass transfer on a stretching sheet with suction or blowing. *Can. J. Chem. Engng.* 55: 744-746.
- HIEMENZ, K. 1911. Die Grenzschicht an einem in den gleichformigen Flussigkeitsstrom eingetauchten geraden Kreiszyylinder. *Dingl. Polytech. J.* 32: 321-410.
- ISHAK, A., R. NAZAR and I. POP. 2006a. Magnethydrodynamic stagnation-point flow towards a stretching ventical sheet. *Magneto hydrodynamics* 42: 17-30.
- ISHAK, A., R. NAZAR and I. POP. 2006b. Mixed convection boundary layers in the stagnation-point flow toward a stretching vertical sheet. *Meccanica* 41: 509-518.
- ISHAK, A., R. NAZAR and I. POP. 2007a. Mixed convection on the stagnation point flow toward a vertical, continously stretching sheet. *ASME J. Heat Trans.* 129: 1087-1090.
- ISHAK, A., R. NAZAR, N.M. ARIFIN and I. POP. 2007b. Dual solutions in mixed convection flow near a stagnation point on a vertical porous plate. *Int. J. Thermal Sciences* (in press).
- ISHAK, A., R. NAZAR and I. POP. 2007c. Stagnation flow of a micropolar fluid towards a vertical permeable surface. *Int. Comm. Heat Mass Trans.* (in press).
- ISHAK, A., R. NAZAR and I. POP. 2007d. Boundary-layer flow of a micropolar fluid on a continuously moving or fixed permeable surface. *Int. J. Heat Mass Trans.* 50: 4743-4748.
- ISHAK, A., R. NAZAR and I. POP. 2007e. Dual solutions in mixed convection boundary-layer flow with suction or injection. *IMA J. Appl. Math.* 72:451-463.
- ISHAK, A., J.H. MERKIN, R. NAZAR and I. POP. 2007f. Mixed convection boundary layer flow over a permeable vertical surface with prescribed wall heat flux. *Z. ANGEW. Math. Phys.* (online first).
- LOK, Y.Y., N. AMIN, D. CAMPEAN and I. POP. 2005. Steady mixed convection flow of a micropolar fluid near the stagnation point on a vertical surface. *Int. J. Num. Methods Heat Fluid Flow* 15: 654-670.
- MAGYARI, E. and B. KELLER. 2000. Exact solution for self-similar boundary-layer flows induced by permeable stretching surfaces. *Eur. J. Mech. B-Fluids* 19: 109-122.
- MAHAPATRA, T.R. and A.S. GUPTA. 2001. Magneto hydrodynamic stagnation-point flow towards a stretching sheet. *Acta Mech.* 152: 191-196.
- MAHAPATRA, T.R. and A.S. GUPTA. 2002. Heat transfer in stagnation-point flow towards a stretching sheet. *Heat Mass Trans.* 38: 517-521.
- NAZAR, R., N. AMIN, D. FILIP and I. POP. 2004a. Stagnation point flow of a micropolar fluid towards a stretching sheet. *Int. J. Nonlinear Mech.* 39: 1227-1235.
- NAZAR, R., N. AMIN, D. FILIP and I. POP. 2004b. Unsteady boundary layer flow in the region of the stagnation point on a stretching sheet. *Int. J. Engng. Sci.* 42: 1241-1253.
- RAMACHANDRAN, N., T.S. CHEN and B.F. ARMALY. 1988. Mixed convection in stagnation flows adjacent to vertical surface. *J. Heat Trans.* 110: 373-377.
- WATANABE, T. 1991. Forced and free convection boundary layer flow with uniform suction or injection on a vertical flat plate. *Acta Mech.* 89: 123-132.